Contents list available at IJRED website

Int. Journal of Renewable Energy Development (IJRED)

Journal homepage: http://ejournal.undip.ac.id/index.php/ijred

Performance Analysis of Maximum Power Point Tracking Algorithms Under Varying Irradiation

Bhukya Krishna Naick[a*], Tarun Kumar Chatterjee[b], and Kalyan Chatterjee[c]

[a,c] *Department of Electrical Engineering, IIT(ISM), Dhanbad, Jharkhand, India – 826004.*

[b] *Department of Mining Machinery Engineering, IIT(ISM), Dhanbad, Jharkhand, India – 826004.*

ABSTRACT. Photovoltaic (PV) system is one of the reliable alternative sources of energy and its contribution in energy sector is growing rapidly. The performance of PV system depends upon the solar insolation, which will be varying throughout the day, season and year. The biggest challenge is to obtain the maximum power from PV array at varying insolation levels. The maximum power point tracking (MPPT) controller, in association with tracking algorithm will act as a principal element in driving the PV system at maximum power point (MPP). In this paper, the simulation model has been developed and the results were compared for perturb and observe, incremental conductance, extremum seeking control and fuzzy logic controller based MPPT algorithms at different irradiation levels on a 10.2 kW PV array. The results obtained were analysed in terms of convergence rate and their efficiency to track the MPP.

Keywords: Photovoltaic system, MPPT algorithms, perturb and observe, incremental conductance, scalar gradient extremum seeking control, fuzzy logic controller.

Article History: Received 3rd Oct 2016; Received in revised form 6th January 2017; Accepted 10th February 2017; Available online
How to Cite This Article: Naick, B. K., Chatterjee, T. K. & Chatterjee, K. (2017) Performance Analysis of Maximum Power Point Tracking Algorithms Under Varying Irradiation. Int. Journal of Renewable Energy Development, 6(1), 65-74.
http://dx.doi.org/10.14710/ijred.6.1.65-74

1. Introduction

In addition to conventional energy sources, the contribution of alternative sources of energy has significantly marked up in generation of electrical power throughout the world. Progressive research and development in the field of power electronics has made these alternative energy sources to be competent enough to generate electrical energy at lower cost. In alternative energy sources, generation of power by using solar PV array has gained wide popularity because of availability of solar insolation round the year throughout the day time. To harness maximum energy from solar insolation at different irradiation levels, the PV array should be driven at maximum power point (MPP). Some established topologies of dc to dc converter along with maximum power point tracking (MPPT) controller may be used to drive the PV array at MPP.

Various MPPT algorithms are existing and have been employed in MPPT controllers. The most famous traditional MPPT algorithms are perturb & observe (P&O) and incremental conductance (INC) algorithms (Femia *et al.* 2015, Liu *et al.* 2008). Artificial neural network (ANN) and fuzzy logic controller (FLC) based MPPT algorithms are considered to be part of artificial intelligent (AI) techniques (Lin *et al.* 2011, Khateb *et al.* 2014). The MPPT algorithms based on nature inspired optimization techniques are genetic algorithm (Larbes *et al.* 2009), particle swarm optimization technique (Liu *et al.* 2012), ant colony optimization (Jianga *et al.* 2013), artificial bee colony (Benyoucef *et al.* 2015), and grey wolf optimization technique (Mohanty *et al.* 2016). The P&O method is easier to implement, but this algorithm fails to track MPP and will result in oscillation at steady state point. To improve tracking efficiency and to reduce oscillations, a changeable step size P&O approach has been presented in (Ahmed *et al.* 2015). The performance of INC method is quite good when compared to that of P&O method, but its response time depends upon the constant or changeable step size. The constant step size in INC method will slow down the

* Corresponding author: krishnalalitha.b@gmail.com

response of MPPT controller, but its response will be faster with changeable step size (Tey *et al.* 2014).

The computational intelligence algorithms like ANN and FLC are more efficient and faster in tracking MPP when compared to that of conventional algorithms. Instead of using complicated neural network, a simple and highly efficient single neural control scheme was proposed in (Kofinas *et al.* 2015). The classification of ANN based MPPT techniques were analyzed in (Elobaid *et al.* 2015) and these techniques are dependent on the type of input to the controller. An adaptive FLC was proposed in (Guenounou *et al.* 2014), which is a combination of the two separate rule bases and a gain attached to the MPPT controller, resulting in improved performance. The first rule base will adjust the duty cycle and the second rule base will be controlling the controller's gain. The tracking efficiency obtained in a PSO based MPPT controller was 99.93% when compared to tracking efficiency of 55.05% obtained by P&O MPPT controller (Oliveira *et al.* 2016). In this method, the global MPP (GMPP) has been tracked by PSO algorithm whereas the P&O algorithm tracks the local MPP (LMPP) only. The time taken to track the LMPP by P&O algorithm was very less when compared to the time taken to track the GMPP by PSO algorithm.

In ant colony optimization technique based MPPT controller (Jianga *et al.* 2013), the tracking efficiency is quite good for slow changes in irradiation level, whereas, the tracking efficiency is very poor for rapidly changing irradiation levels. An artificial bee colony optimization technique based MPPT controller has been implemented in (Fathy *et al.* 2015) to track the GMPP and to mitigate power loss in shaded modules of PV array. An extremum seeking control (ESC) system proposed in (Leyva *et al.* 2006), is a self-tuning algorithm and it has been implemented to reduce the oscillations at MPP. The existing ESC based algorithms are adaptive ESC (Li *et al.* 2013), ripple based ESC (Bazzi *et al.* 2011), multivariable newton based ESC (Ghaffari *et al.* 2014), fractional order ESC (Malek *et al.* 2013). From the ESC based methods, it has been observed that the oscillation still exists at MPP region but the level of oscillation is very less in comparison to P&O method. For the constant and varying irradiations, a detailed study of the existing MPPT algorithms were described in (Saravanan *et al.* 2016).

In this paper, the simulation and comparison of four MPPT algorithms have been presented. Out of the four, two are the traditional algorithms called P&O and INC method, whereas the remaining two algorithms are based on recent methods called FLC and scalar gradient extremum seeking control (SGESC) method. The results were compared in terms of efficient tracking of MPP at different irradiation levels and the time taken to reach the MPP for every change in irradiation level.

With this brief introduction, the remaining part of the paper has been organized in the following sequence. Section 2 deals with the modelling of PV module. The P&O, INC, SGESC and FLC methods will be described in section 3. The implementation of simulation model and the obtained results were discussed in section 4.

2. Modeling of Solar PV Cell

Solar PV cell is a simple photo diode consisting of p-type and n-type semiconductor material that produces power, when exposed to the solar irradiation. The physical model of solar PV cell may be represented in the form of single diode or two diode equivalent model by using mathematical equations. These physical models were used to explain the electrical behaviour of PV cell. The single diode equivalent model as shown in Fig. 1 has been simulated in this paper because of ease in implementation and less complexity.

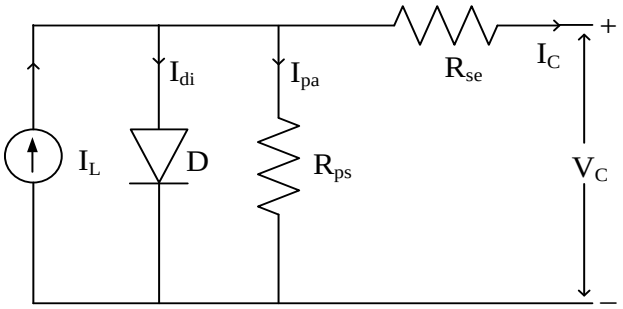

Figure 1 Single diode equivalent model.

The PV model has been implemented by using the equations provided in (Villalva *et al.* 2009). At the output, the current obtained due to illumination of solar irradiation is given by equations (1) and (2).

$$I_C = I_L - I_{di} - I_{pa} \quad (1)$$

$$I_C = I_L - I_{0d}\left[exp\left(\frac{V_C + I_C R_{se}}{V_t a}\right) - 1\right] - \frac{V_C + I_C R_{se}}{R_{ps}} \quad (2)$$

Whereas, I_L (A) is the current generated by solar PV cell due to incident solar irradiation. In equivalent model, I_{di} is the current flowing through diode and I_{pa} (A) is the current flowing through shunt resistance. I_{od} (A) is the leakage current or reverse saturation current. V_c (V) is the output voltage of module. a is the ideality factor of diode. R_{se} (Ω) and R_{ps} (Ω) represents the equivalent resistance of PV module connected in series and shunt. The thermal voltage of PV module is represented by V_t and is given by $V_t = N_S kT_0/q_e$. The number of cells that are connected in series in a string of PV module is stated by Ns.k is the Boltzmann constant (and is equal to $1.3806503.10^{-23}$ J/K), To (in Kelvin) is the temperature at p-n junction, q_e is the electron charge and its value is $1.60217646.10^{-19}$C.

Due to incident solar irradiation, the current

generated by photo diode is given in equation (3).

$$I_L = \left(I_{psc} + K_I \Delta_T\right)\frac{G}{G_n} \quad (3)$$

Whereas, I_{psc} (A) is the current under short circuit conditions or the current generated by PV module at nominal temperature of 25°C and standard solar irradiation of 1000 W/Sq.m. The temperature coefficient under short circuit conditions of PV module is represented by K_I (A/K). The difference between operating temperature To and nominal temperature T_n (in kelvin) is represented by ΔT and is stated by $\Delta T=To-T_n$.G (in W/Sq.m) is the solar irradiation at normal operating conditions and G_n (in W/Sq.m) is the irradiation at nominal temperature. The diode reverse saturation current is dependent upon temperature and is expressed by equation (4).

$$I_0 = I_{n0}\left(\frac{T_n}{T_0}\right)^3 exp\left[\frac{qE_g}{ak}\left(\frac{1}{T_n} - \frac{1}{T_0}\right)\right] \quad (4)$$

The bandgap energy of semiconductor material is represented by Eg (eV) and its value is 1.12 eV for polycrystalline silicon at 25°C. I_{no} (A) is the saturation current at nominal temperature and is expressed by Equation 5.

$$I_{n0} = \frac{I_{psc}}{exp\left(V_{poc}/a\ V_{nt}\right) - 1} \quad (5)$$

V_{poc} (V) is the open circuit voltage at nominal temperature and V_{nt} (V) is the thermal voltage produced by N_s cells connected in series in one string of module at nominal temperature.

3. Maximum Power Point Tracking

As the insolation of sun varies from time to time, the dc to dc converter plays a crucial role in driving the PV array at MPP. As stated in maximum power transfer theorem, the load will receive its peak power, if the value of load impedance is equivalent to complex conjugate of internal impedance of the supply system. So, to drive the PV array at MPP, the load impedance and internal impedance should be matched. The internal resistance of PV module will vary with respect to the varying insolation. The load resistance will be matched with internal resistance of PV module by using dc to dc converter in association with MPPT controller and it has been implemented in this paper. The MPPT controller will produce a suitable value of duty cycle that will be fed to the pulse width modulation (PWM) generator, which produces required triggering signal for the switch present in dc to dc converter.

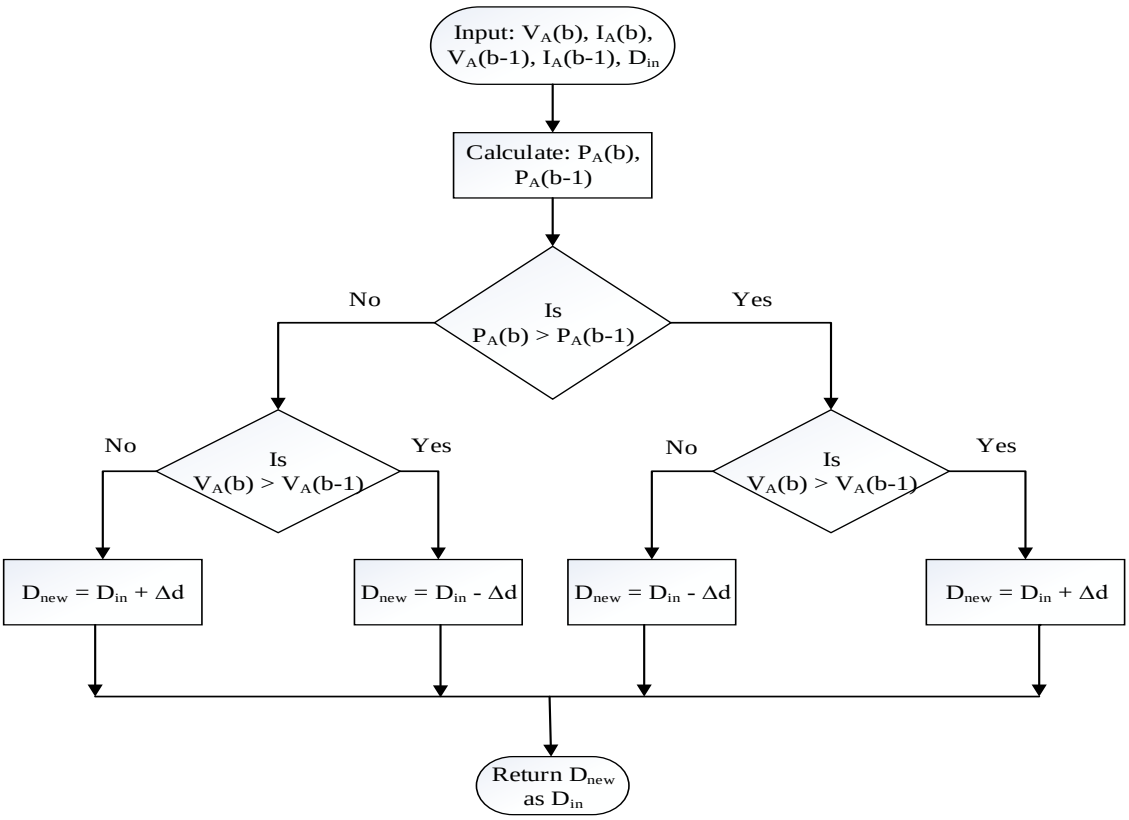

Figure 2 Flow diagram of P&O algorithm.

The purpose of dc to dc converters is to elevate or to lessen the PV voltage to a suitable value, so that the PV system may be interfaced to the grid or load. The dc to dc converters like buck, boost, buck-boost and cuk are existing and a suitable converter may be selected according to the application. For high voltage applications, boost converter is considered to be best one and in this paper, it has been simulated for increasing the PV voltage. The input voltage V_{id}, output voltage V_{od} and duty cycle d are related by using equation (6) (Dileep *et al.* 2015).

$$V_{od} = \frac{V_{id}}{(1-d)} \quad (6)$$

3.1 Perturb & Observe Algorithm

The P&O algorithm as mentioned in (Femia *et al.* 2005, Zainuri *et al.* 2014) has been implemented and it is assumed to be the oldest and traditional MPPT algorithm. The current I_A and voltage V_A of PV array at present step (b^{th}) and the previous step ($(b-1)^{th}$) will be measured. Further, the power at present step $P_A(b)$ and previous step $P_A(b-1)$ will be calculated. If the power at present step $P_A(b)$ is greater than that of power at previous step $P_A(b-1)$ and if the voltage $V_A(b)$ is greater than that of $V_A(b-1)$, then the tracking will continue on the left side of MPP, by increasing the duty factor with a small value. At the same time, if the power $P_A(b)$ is less than that of $P_A(b-1)$ and if the voltage $V_A(b)$ is greater than that of $V_A(b-1)$, then the tracking will continue on the right side of MPP by decreasing duty cycle with a small value. The flow diagram is shown in Fig. 2.

The privilege of this algorithm is that it is easier to implement and also the cost is low. The disadvantage associated with the algorithm is that it never tracks the optimal value and there will be always having oscillation near to the optimal value of MPP. The improvement in this method has been proposed in (Dileep *et al.* 2015, Piegari *et al.* 2010).

3.2 Incremental Conductance Algorithm

The INC algorithm depends upon reality that the differentiation of PV power (at MPP) with respect to voltage is equal to zero and it also depends upon the slope of P-V characteristics.

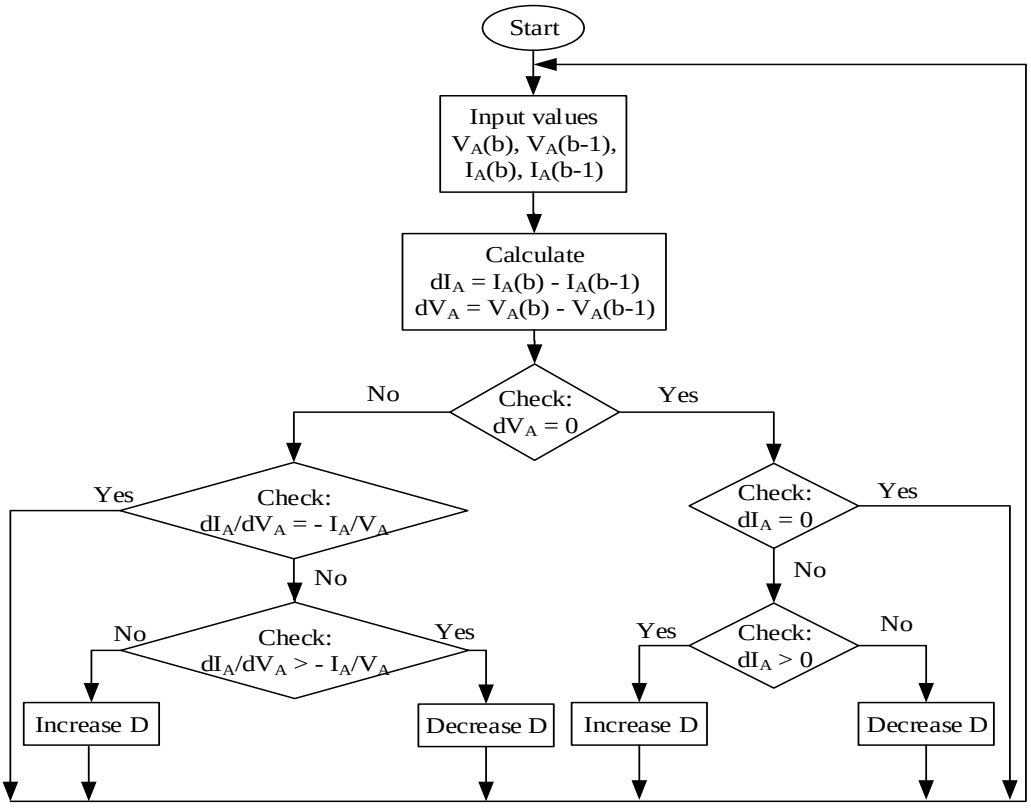

Figure 3 Flow diagram of INC algorithm.

The implementation of INC algorithm may be explained by using the following equations as in (Eltawil *et al.* 2013).

$$\frac{dP_A}{dV_A} = \frac{d(V_A I_A)}{dV_A} = I_A + V_A \frac{dI_A}{dV_A} = 0 \quad (7)$$

The equation (7) is the condition at MPP and also it

may be written as

$$-\frac{I_A}{V_A} = \frac{dI_A}{dV_A} \quad (8)$$

The left hand component in equation (8) indicates the instantaneous conductance of PV array, but in opposite direction, whereas, the right hand component indicates the incremental conductance at MPP. The other conditions for tracking MPP on the slope of P-V characteristics are given by the equations (9) and (10).

$$\frac{dI_A}{dV_A} > -\frac{I_A}{V_A} \quad (9)$$

$$\frac{dI_A}{dV_A} < -\frac{I_A}{V_A} \quad (10)$$

Equation (9) represents the condition of (dI_A/dV_A)>0and it also indicates that the driving point is lying on the left side of MPP. Whereas, the eq (10) represents the condition of (dI_A/dV_A)<0and also indicates that the driving point is on right side of MPP. Based on the above statements, the flow diagram of INC algorithm (Eltawil *et al.* 2013) is shown in Fig. 3 and the same was implemented in this paper.

As the algorithm starts, the current value of the voltage & current will be measured and from the preceding cycle, the previous value of the voltage & current will be obtained. Further the values of dV_A and dI_A will be calculated. If there is no change in the solar irradiation and if the values of dV_A and dI_A are equal to zero, then the algorithm is tracking MPP. If the value of dV_A is equal to zero and dI_A is greater than zero, then it indicates that there is rise in solar irradiation causing the algorithm to increase the value of MPP. Similarly if the value of dV_A is equal to zero and dI_A is less than zero, then it indicates that there is decrease in solar irradiation, initiating the algorithm to lower the MPP. In this way, the driving point will be moving on the slope present on either side of MPP, till it reaches the optimal value of MPP. The demerit of this algorithm is that it is little bit more complicated when compared to that of P&O algorithm, but the tracking efficiency is quite good under varying insolation levels. Also, the response time for tracking the optimal value of MPP depends upon the value of fixed step size used in this algorithm. The improvement in this algorithm is the introduction of variable step size, as proposed in (Liu *et al.* 2008).

3.3 Scalar Gradient based Extremum Seeking Control (SGESC)

The ESC method based MPPT has been proposed to reduce the oscillations at steady state point and to track an extremum value on P-V characteristics (Leyva *et al.* 2006). Based on ESC method, the other technique proposed is the sinusoidal ESC (SESC) (Leyva *et al.* 2012). With a small modification in gradient detector, it is also called as scalar gradient based ESC (SGESC) (Ghaffari *et al.* 2015) and this technique has been implemented. Though the method has been explained clearly in the cited references, it has been presented here in brief for understanding purpose. The main components of the SGESC method are power from P-V characteristics, gradient detector consisting of high pass filter and low pass filter, a small sinusoidal perturbation signal with a and ω as its amplitude and frequency as shown in Fig. 4.

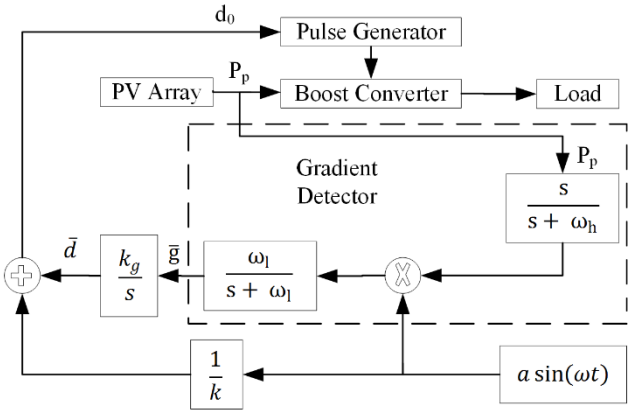

Figure 4 Block diagram of SGESC.

The input and output parameters of SGESC are PV power P_P and the duty factor d_0. The duty factor d_0 will drive the dc to dc converter, which in turn will drive PV array at MPP. The power P_P will be fed as input to the gradient detector and the dc components present in the input signal will be removed by passing it through high pass filter.

Depending upon the resultant sinusoidal signal obtained from the high pass filter, it may be estimated that the duty factor d_0, which has been fed as input to dc-dc converter was greater than or less than the optimal value of duty factor d^* (duty factor at MPP). If the resultant signal is in phase with small sinusoidal perturbation then it indicates that the fed duty factor d_0 was greater than the optimal value d^* and if it is out of phase, then it indicates that the duty factor d_0 was less than the optimal value d^*. If the fed duty factor d_0 is equal to the optimal value d^*, then the resultant signal will have frequency double than that of frequency of small sinusoidal perturbation. To obtain the gradient function g, the resultant sinusoidal signal from the high pass filter will be multiplied with the a.sin(wt)/k and then it will passed through low pass filter to remove dc components.

The gradient function g will act as input to the integrator and the duty factor dwill be obtained as output. Further, the duty factor d will be multiplied with

small sinusoidal perturbation and d_0 will be obtained as a product, which will be supplied to the dc to dc converter. The frequencies of low pass filter ω_l, high pass filter ω_h and small sinusoidal perturbation ω may be chosen in such a manner that $\omega_h \leq \omega_l << \omega$ as in (Ghaffari *et al.* 2015).

3.4 FLC based MPPT controller

FLC, a non-linear controller, will give the logical response as an output to the non-linear behaviour of the input. The two design methods available in FLC are Mamdani (M) and Tagachi-Sukeno (T-S) methods. In the present work, mamdani method based FLC has been implemented. The different levels involved in FLC process are fuzzification, rule base fuzzy inference system and defuzzification process (Bendib *et al.* 2015).

Fuzzification is a process of converting the true values (also called crisp values) of input parameters into fuzzy membership functions. The limits of input and output parameters have been defined by using five linguistic variables called as NH (negative higher), NL (negative lower), ZR (zero), PL (positive lower), PH (positive higher) and will be represented in the form of triangular membership functions. The fuzzy membership functions will be further processed by using the rule base fuzzy inference system and in this process, a set of 25 rules have been framed which is a combination of input and output fuzzy membership functions. After that, the processed output membership functions will be converted back into crisp output values by using defuzzification process. Max criterion Method (MCM), mean of maxima (MOM), center of area (COA) are the methods available to perform the defuzzication process. In this paper, the COA method has been used and the output value will be calculated by using the following equation (11).

$$\Delta D(k) = \frac{\sum_{j=1}^{n} \mu\left(\Delta D_j(k)\right) X \Delta D_j(k)}{\sum_{j=1}^{n} \mu\left(\Delta D_j(k)\right)} \quad (11)$$

The input to the FLC are error value 'er' and the difference in error value 'der', given by the equations (12) and (13).

$$er = \frac{dP_p}{dV_p} \quad (12)$$

$$der = er\,(b) - er\,(b-1) \quad (13)$$

Table 1
Rules of fuzzy logic controller.

		der				
		NH	NL	ZE	PL	PH
er	NH	NH	NH	NL	NL	ZE
	NL	NH	NL	NL	ZE	PL
	ZE	NL	NL	ZE	PL	PL
	PL	NL	ZE	PL	PL	PH
	PH	ZE	PL	PL	PH	PH

The value of error 'er' is the differentiation of power with respect to voltage and 'der' is the difference between the errors at bth position and (b-1)th position. The output of FLC based MPPT controller is the duty factor 'd_0'.

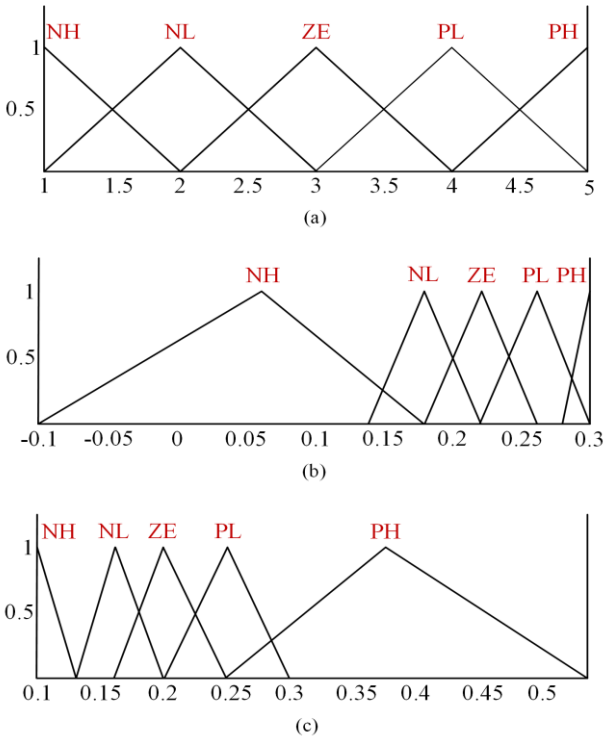

Figure 5 Membership functions of (a) error 'er', (b) change in error 'der' (c) duty factor 'd_0'.

The set of rules used in fuzzy inference system is shown in Table 1 and the Fig. 5 exhibits the membership functions of 'er', 'der' and 'D_0'.

4. Simulation and Results

The PV array with output power of 10.2 kW has been simulated in MATLAB/SIMULINK platform. The solar PV module with different power rating supplied by various manufacturers, are available in the market. KC200GT solar PV module has been considered in present study and its parameters are given in Table 2 (Villalva *et al.* 2009).

Table 2
KC200GT parameters.

Open Circuit Voltage	32.9 V
Short Circuit Current	8.21 A
Diode Ideality Factor	1.3
Short Circuit Current temperature coefficient	0.0032 A/K
Series Resistance	0.221 Ω
Shunt Resistance	415.405 Ω
Number of cells in module	54

Table 3
Other parameters used in the model.

Inductance of Boost Converter L_b	3.636 mH
DC Link Capacitance	10000 µF
Nominal DC bus voltage	500 V

Since, the KC200GT PV module is capable of supplying power of 200W only, few similar modules will be connected in sequence to increase the PV output voltage and to form a string. At the same time, these strings will be connected in shunt to elevate the output current and power. The number of modules that are connected in sequence of a string is represented by N_{ss}, whereas the number of shunt strings in an array are represented by N_{pp}. The boost type dc to dc converter suitable for high voltage applications has been implemented to drive the PV array at MPP. The other variables used in the simulation model are shown in Table 3.

As explained earlier, the P&O, INC, FLC and SGESC based MPPT algorithms were implemented and the results have been presented for varying irradiance. A value of 0.01 has been used for perturbation in P&O algorithm, to perturb the value of duty factor d and the same value has been considered as a fixed step size in INC algorithm to increment or decrement the value of duty factor d_0. The duty factor d_0 will be obtained directly as an output of the FLC based MPPT controller. The value of frequencies in high pass filter, low pass filter and small sinusoidal perturbation in SGESC based MPPT controller are 70 rad/sec, 80 rad/sec and 110 rad/sec. The results that has been obtained were compared and presented as follows.

To validate the simulation model of PV array, the current vs voltage and power vs voltage curves has been plotted. The I-V curves at temperature levels of 25°C, 50°C, 75°C is shown in Fig. 6 (a). It may be observed that the output voltage of PV array decreases with the increase in temperature, whereas, the output current deviates with a small value from its original value. As a result, the output power of PV array will decrease as shown in Fig. 6 (b).

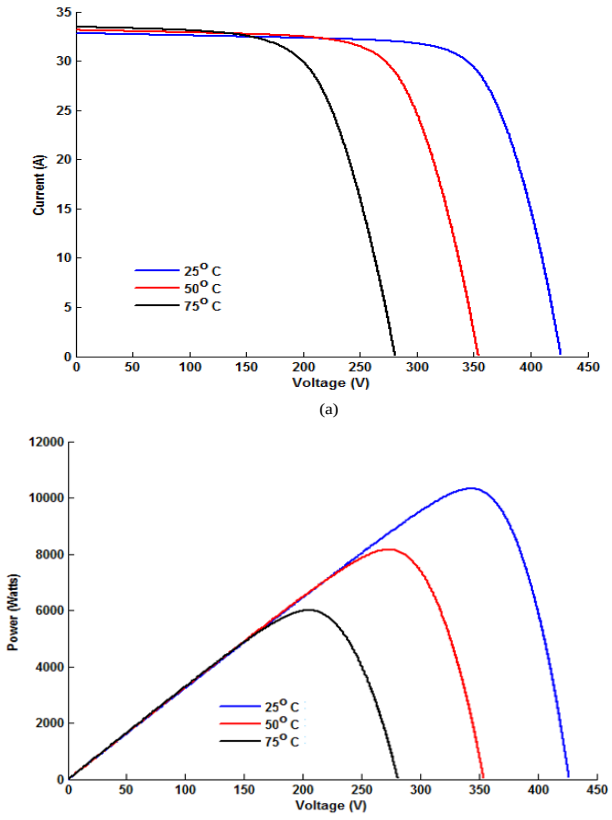

Fig. 6 (a) I-V curve and (b) P-V curve at different temperature levels.

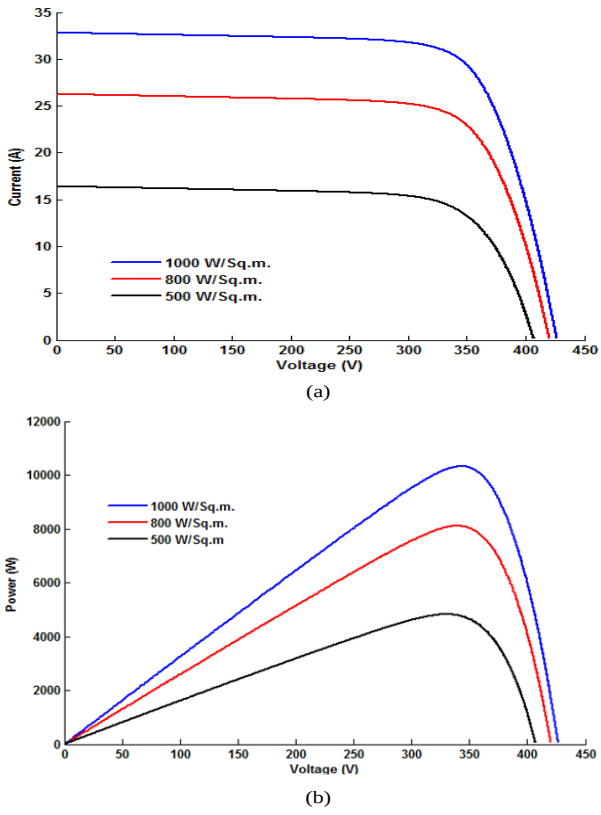

Figure 7 (a). I-V curve and (b). P-V curve at different irradiation levels.

The effect of change in irradiation on I-V curves is shown in Fig. 7 (a). The irradiation levels of 1000 W/Sq.m, 800 W/Sq.m and 500 W/Sq.m has been considered for simulation. The output current of PV array will decrease due to decrease in irradiation causing the power of PV array to decrease as shown in Fig. 7 (b).

The input parameters which will control the output power of PV array are solar irradiation and temperature. To analyze and compare the results obtained from the above mentioned MPPT algorithms in terms of tracking efficiency, a varying irradiation level of solar insolation has been fed to PV array. The output power tracked by the MPPT controllers are shown in Fig. 8.

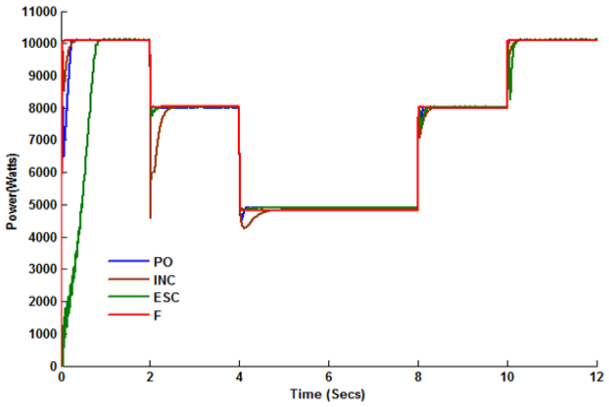

Figure 8 Output power curves of PV array.

As shown in Fig. 8, the four MPPT algorithms are approximately tracking the same amount of power at MPP, but there is difference in the tracking time and tracking efficiency. The time taken to track MPP and the value of power tracked by four algorithms for varying irradiation is shown in Table 4. In this table, P&O stands for perturb and observe method, INC stands for incremental conductance method, ESC stands for scalar gradient based extremum seeking control method, F stands for fuzzy logic controller.

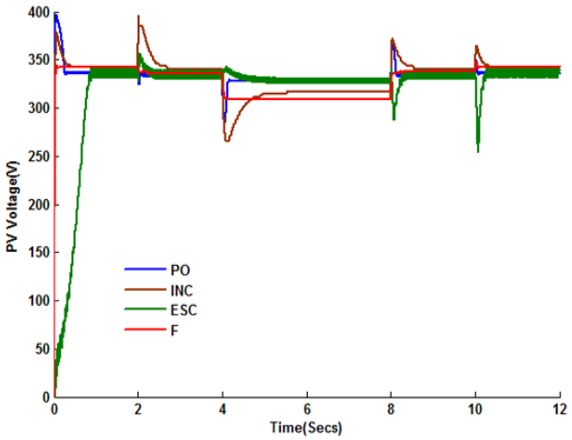

Figure 9 PV output voltage curves.

Table 4
Comparison of algorithms in terms of tracking time.

Irradiation level and simulation time applied as input to PV array		1000 W/Sq.m from 1 to 2 Secs	800 W/Sq.m from 2 to 4 Secs	500 W/Sq.m from 4 to 8 Secs	800 W/Sq.m from 8 to 10 Secs	1000 W/Sq.m from 10 to 12 Secs
Peak value of power (in Watts) tracked by different MPPT methods. Power tracking time (in Seconds) by different MPPT methods.						
P&O	Pmax	**10110**	8010	4894	8010	**10110**
	Time	0.25	**0.05**	0.15	0.15	**0.06**
INC	Pmax	10105	8023	4868	8023	10105
	Time	0.35	0.45	0.8	0.37	0.3
ESC	Pmax	10108	8031	**4900**	**8031**	10108
	Time	0.85	0.25	0.35	0.3	0.25
FLC	Pmax	10102	**8037**	4811	8002	10102
	Time	**0.05**	0.07	**0.07**	**0.03**	0.09

Table 5
Comparison of algorithms in terms of tracking efficiency.

Irradiation level	1000 W/Sq.m	800 W/Sq.m	500 W/Sq.m
Maximum power obtained from P-V characteristics in Watts	10330	8115	4928
Maximum power in Watts tracked by each MPPT method and tracking efficiency in %			
P&O	**10110, 97.87**	8010, 98.7	4894, 99.31
INC	10105, 97.82	8023, 98.86	4868, 98.78
ESC	10108, 97.85	8031, 98.96	**4900, 99.43**
FLC	10102, 97.79	**8037, 99.03**	4811, 97.63

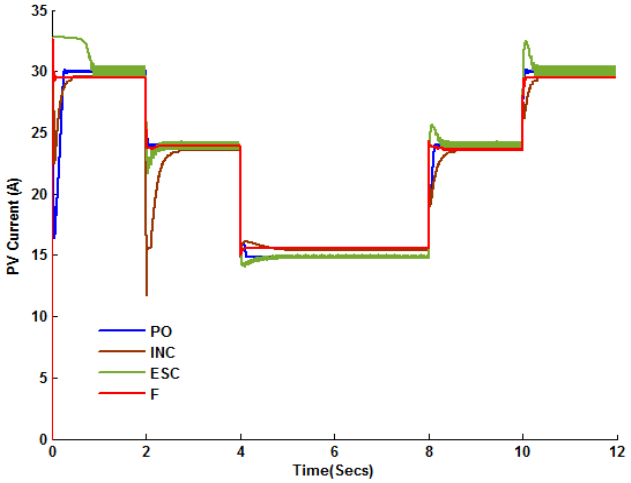

Figure 10 PV output current curves.

Of all methods, FLC proves to be faster in tracking the MPP for varying irradiation levels though the power tracked is almost equal to the power tracked by other methods. The comparison in terms of tracking efficiency of these algorithms are given in Table 5.

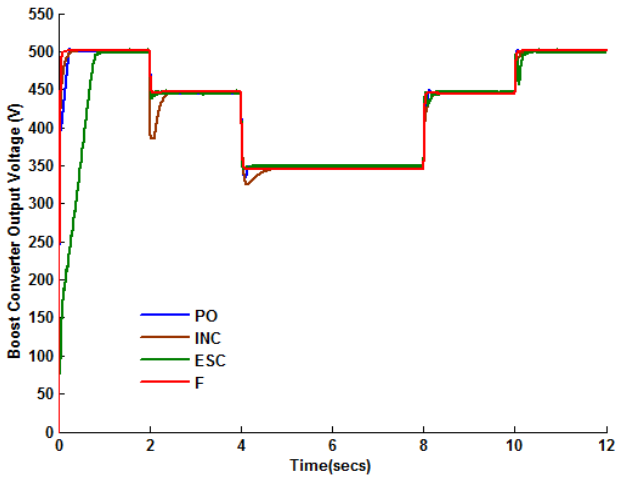

Fig. 11 Boost converter output voltage curves.

The output voltage and current curves of PV array are shown in Fig. 9 and Fig. 10. In the figures, it may be observed that with the change in irradiation level, the output voltage of PV array decreases with a small value but the output current gets more effected leading to decrease in PV output power. The variation of boost converter voltage due to change in output voltage of the PV array is shown in Fig. 11. The output voltage of the boost converter also gets effected due to change in output voltage of PV array and also due to change in duty factor. The variation of duty factor is shown in Fig. 12.

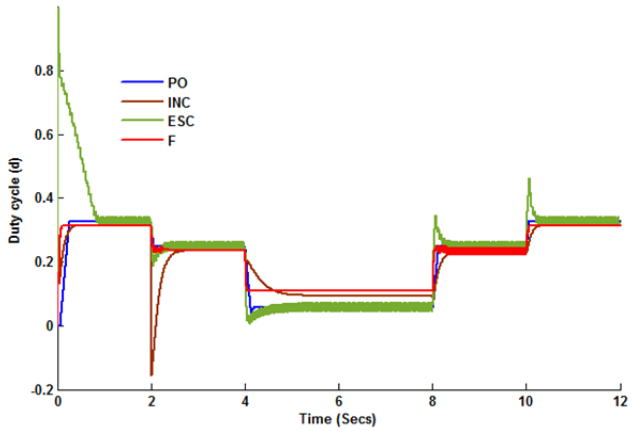

Fig. 12 Variation of duty factor.

The P&O and ESC based MPPT controllers are similar in behaviour, but there are oscillations in the PV output voltage, current, boost converter output voltage and duty factor in ESC method due to small sinusoidal perturbation. The performance of INC and FLC based MPPT controllers are similar in nature but the transient time of INC is more when compared to FLC. The summary of the tracked values of PV output voltage, PV current, boost converter output voltage and duty factor from the P&O, INC, SGESC and FLC algorithms based MPPT controllers are presented in Table 6.

Table 6
Comparison of different characteristics exhibited by the four algorithms.

Irradiation level	1000 W/Sq.m	800 W/Sq.m	500 W/Sq.m
PV output voltage in Volts			
P&O	337	335	328
INC	342	**341**	317
ESC (avg)	337	337	**329**
F	**342.5**	335.8	309.2
PV output current in Amps			
P&O	**30**	**24**	14.9
INC	29.6	23.55	15.35
ESC (avg)	**30**	**24**	14.9
F	29.5	23.95	**15.55**
Boost converter output voltage in Volts			
P&O	**501**	446	348.5
INC	500.8	446.2	347.5
ESC (avg)	**501**	**446.5**	**349**
F	500.5	**446.5**	345.5
Duty factor (d)			
P&O	0.327	0.249	0.058
INC	0.315	0.235	0.092
ESC (avg)	**0.33**	**0.25**	0.06
F	0.312	0.239	**0.11**

From the above implemented MPPT methods, FLC based MPPT controller is found to be the best one for varying irradiations, because it tracks the optimal value of MPP in a very short time.

5. Conclusion

In this paper, PV array along with P&O, INC, SGESC and FLC based MPPT controllers has been simulated to study their behaviour under the conditions of varying irradiance. The behaviour of the algorithms was observed in terms of tracking time, tracking efficiency and optimal value of MPP for varying irradiance. The irradiance to the input of PV array has been reduced from nominal value of 1000 W/Sq.m to half of its value of 500 W/Sq.m along with an intermediate value of 800 W/Sq.m and subsequently it has been increased to the same nominal values of irradiance. Though the P&O method is a less complicated when compared to other methods, but it has been observed that the FLC based MPPT controller rapidly tracks the MPP with minimum oscillations at MPP.

References

Ahmed, J. & Salam, Z. (2015) An improved perturb and observe (P&O) maximum power point tracking (MPPT) algorithm for higher efficiency. *Applied Energy*, 150, 97–108.

Bazzi, A. M. & Krein. P. T. (2011) Concerning "Maximum Power Point Tracking for Photovoltaic Optimization Using Ripple-Based Extremum Seeking Control". *IEEE Trans. on Power Electronics*, 26 (6), 1611-1612.

Bendib, B., Belmili, H. & Krim, F. (2015) A survey of the most used MPPT methods: Conventional and advanced algorithms applied for photovoltaic systems. *Renewable and Sustainable Energy Reviews*, 45, 637–648.

Benyoucef, A. S., Chouder, A., Kara, K., Silvestrec, S. & saheda, O. A. (2015) Artificial bee colony based algorithm for maximum power point tracking (MPPT) for PV systems operating under partial shaded conditions. *Applied Soft Computing*, 32, 38–48.

Dileep, G. & Singh, S. N. (2015) Maximum power point tracking of solar photovoltaic system using modified perturbation and observation method. *Renewable and Sustainable Energy Reviews*, 50, 109–129.

Elobaid, L. M., Abdelsalam, A. k. & Zakzouk, E. E. (2015) Artificial neural network-based photovoltaic maximum power point tracking techniques: a survey. *IET Renewable power Generation*, 9(8), 1043-1063.

Eltawil, M. A. & Zhao, Z. (2013) MPPT techniques for photovoltaic applications. *Renewable and Sustainable Energy Reviews*, 25, 793–813.

Fathy, A. (2015) Reliable and efficient approach for mitigating the shading effect on photovoltaic module based on Modified Artificial Bee Colony algorithm. Renewable Energy, 81, 78-88.

Femia, N., Petrone, G., Spagnuolo, G. & Vitell, M. (2005) Optimization of Perturb and Observe Maximum Power Point Tracking Method. *IEEE Trans. Power Electronics*, 20(4), 963-973.

Ghaffari, A., Krsti´c, M. & Seshagiri, S. (2014) Power Optimization for Photovoltaic Microconverters Using Multivariable Newton-Based Extremum Seeking. *IEEE Trans. Control Systems Technology*, 22 (6), 2141-2149.

Ghaffari, A., Seshagiri, S. & Krstić, M (2015) Multivariable maximum power point tracking for photovoltaic micro-converters using extremum seeking. *Control Engineering Practice*, 35, 83–91.

Guenounou, O., Dahhou, B. & Chabour, F. (2014) Adaptive fuzzy controller based MPPT for photovoltaic systems. *Energy Conversion and Management*, 78, 843–850.

Jianga, L. L., Maskell, D.L. & Patra. J.C. (2013) A novel ant colony optimization-based maximum power point tracking for photovoltaic systems under partially shaded conditions. *Energy and Buildings*, 58, 227–236.

Khateb, A. E., Rahim, N.A., Selvaraj, J. & Uddin, M.N. (2014) Fuzzy-Logic-Controller-Based SEPIC Converter for Maximum Power Point Tracking. *IEEE Trans. Industry Applications*, 50(4), 2349-2358.

Kofinas, P., Dounis, A. I., Papadakis, G. & Assimakopoulos, M. N. (2015) An Intelligent MPPT controller based on direct neural control for partially shaded PV system. *Energy and Buildings*, 90, 51–64.

Larbes, C., Aï¨t Cheikh, S, M., Obeidi, T. & Zerguerras, A. (2009) Genetic algorithms optimized fuzzy logic control for the maximum power point tracking in photovoltaic system. *Renewable Energy*, 34(10), 2093–2100.

Leyva, R., Alonso, C., Queinnec, I., Cid-Pastor, A., Lagrange, D. & Martínez-Salamero, L. (2006) MPPT of Photovoltaic Systems using Extremum–Seeking Control. *IEEE Trans. Aerospace and Electronic Systems*, 42 (1), 249-258.

Leyva, R., Olalla, C., Zazo, H., Cabal, C., Cid-Pastor, A., Queinnec, I. & Alonso, C. (2012) MPPT Based on Sinusoidal Extremum-Seeking Control in PV Generation. *International Journal of Photoenergy*, 2012(Article ID 672765), 7 pages.

Li, X., Li, Y. & Seem, J. E. (2013) Maximum Power Point Tracking for Photovoltaic System Using Adaptive Extremum Seeking Control. *IEEE Trans. Control Systems Technology*, 21(6), 2315-2322.

Lin, W., Hong, C. & Chen, C. (2011) Neural-Network-Based MPPT Control of a Stand-Alone Hybrid Power Generation System. *IEEE Trans. Power Electronics*, 26(12), 3571-3581.

Liu, F., Duan, S., Liu, F., Liu, B. & Kang, Y. (2008) A Variable Step Size INC MPPT Method for PV Systems. *IEEE Trans. Industrial Electronics*, 55(7), 2622-2628.

Liu, Y., Huang, S., Huang, J. & Liang, W. (2012) A Particle Swarm Optimization-Based Maximum Power Point Tracking Algorithm for PV Systems Operating Under Partially Shaded Conditions. *IEEE Trans. Energy Conversion*, 27(4), 1027-1035.

Malek, H., Dadras, S. & Chen, Y. (2013) *An Improved Maximum Power Point Tracking based on Fractional Order Extremum Seeking Control in Grid-Connected Photovoltaic (PV) Systems*. proceedings of the ASME 2013 International Design Engineering Technical Conferences and Computers and Information in Engineering Conference IDETC/CIE 2013, Portland, Oregon, USA, August 4-7, 2013.

Mohanty, S., Subudhi, B. & Ray, P. K. (2016) A New MPPT Design Using Grey Wolf Optimization Technique for Photovoltaic System under Partial Shading Conditions. *IEEE Trans. Sustainable Energy*, 7(1), 181-188.

Oliveira, F. M. D., Silva, S. A. O. D., Durand, F. R., Sampaio, L. P., Bacon, V. D. & Campanhol, L. B. G. (2016) Grid-tied photovoltaic system based on PSO MPPT technique with active power line conditioning. *IET Power Electronics*, 9(6), 1180-1191.

Piegari, L. & Rizzo, R. (2010) Adaptive perturb and observe algorithm for photovoltaic maximum power point tracking. *IET Renewable Power Generation*, 4(4), 317– 328.

Saravanan, S. & Babu, N. R. (2016) Maximum power point tracking algorithms for photovoltaic system – A review. *Renewable and Sustainable Energy Reviews*, 57, 192–204.

Tey, K. S. & Mekhilef, S. (2014) Modified incremental conductance MPPT algorithm to mitigate inaccurate responses under fast-changing solar irradiation level. *Solar Energy*, 101, 333–342.

Villalva, M. G., Gazoli, J. R. & Filho, E. R. (2009) Comprehensive Approach to Modeling and Simulation of Photovoltaic Arrays. *IEEE Trans. Power Electronics*, 24(5), 1198-1208.

Zainuri, M. A. A. M., Radzi, M. A. M., Soh, A. C. & Rahim, N. A. (2014) Development of adaptive perturb and observe-fuzzy control maximum power point tracking for photovoltaic boost dc–dc converter. *IET Renewable Power Generation*, 8(2), 183–194.